

Supplementary Information for

MTSS1/Src family kinase Dysregulation Underlies Multiple Inherited Ataxias

Alexander S. Brown, Pratap Meera, Banu Altindag, Ravi Chopra, Emma Perkins, Sharan Paul, Daniel R. Scoles, Eric Tarapore, Jessica Magri, Haoran Huang, Mandy Jackson, Vikram G. Shakkottai, Thomas S. Otis, Stefan M. Pulst, Scott X. Atwood, Anthony E. Oro

Address correspondence to:

Anthony E. Oro oro@stanford.edu (Lead Contact), Alexander Brown (sale@stanford.edu), or Scott X Atwood (satwood@uci.edu)

This PDF file includes:

Supplemental methods

Figs. S1 to S4

EXPERIMENTAL MODEL AND SUBJECT DETAILS

MIM^{CKO}: MIM^{EX15Loxp} mice were crossed to L7-Cre (89) to generate MIM^{CKO}.

ATXN2^{Q127}: ATXN2^{Q127} mice were previously characterized in (1).

ATXN1^{Q82}: ATXN1^{Q82} mice were previously characterized in (75).

SPTNB2: SPTNB2 null mice were previously characterized in (3).

METHOD DETAILS

Behavior testing:

Rotarod and activity chamber testing was performed by the Stanford Behavioral and Functional Neuroscience Lab. For rotarod mice were trained on 2-20rpm accelerating rod for 4 trials with 15 minute rest intervals between trials. Testing was performed after one rest day at 16rpm constant speed. For activity chamber mice were placed in chamber and measured for 10 minutes 3 times on separate days.

Composite Limb Gait Ledge test was performed as in (46).

Cerebellar dasatinib administration:

Mice were trained on 4-40rpm accelerating rotorod with 15 minute rest intervals. Mice were tested on the same 4-40rpm paradigm after a rest day.

Dasatinib was dissolved in 40% capitsol to a 9mM solution, then diluted in acsf and loaded into azlet pump 1004. Cannulas were inserted at midline, -6.2mm cadual -2.5 DV from bregma. Sutures were closed with ethilon and mice were allowed to recover before subsequent rotarod tests.

Quantitative RT-PCR (QPCR):

QPCR was performed on Trizol extracted total RNA from 3-5 animals per condition using RNA to Ct reagent with the following probes: Mm00479862_g1 (Aif1), Mm00448091_m1 (Sqstrm1), Mm00774656_m1 (Vmp1), Mm99999915_g1 (Gapdh). Fold enrichment was calculated using $2^{-\Delta\Delta Ct}$.

TUNEL assay:

Tunel assay was performed using NeuroTACS in situ apoptosis detection kit (R&D systems) according to manufacturer instructions.

Luciferase assay:

Luciferase activity was measured using *Mtss1* UTR clone S811096 from Switchgear genomics. Constructs were transfected into 293T cells using FugeneHD 48 hours before measurement. For each well of a 96 well plate, 20ng reporter vector was transfected with reported concentration of ATXN2-Q22-flag or ATXN2-Q108-flag constructs. PCDNA was used to normalize transfection amounts.

Luciferase activity was measured on Molecular Dynamics M5 with 1500ms integration time. Nested deletions were constructed by restriction digest, T4 blunting and ligation. Minimal constructs were generated by Gibson assembly.

HEK-293 RNA-IP:

RNA-IP for ATXN2 bound *Mtss1* transcripts in human HEK-293 cells expressing Flag-tagged ATXN2 constructs was performed as in (7).

MTSS1 3'UTR RNA-IP:

293T Cells were lysed in 20mM Tris Ph 7.5, 140mM NaCl, 1mM EDTA, 10% glycerol, 1% Triton X-100, 20mM DTT supplemented with 20U/ml Superase inhibitor (Life), 2U/ml DNase1 (NEB), Complete ultra protease inhibitor tablets (Roche). Flag constructs were immunoprecipitated using Anti-Flag agarose beads (Sigma). RNA was isolated using Trizol (Life) and treated with DNase1 (NEB) for 30 minutes. QRT-PCR was performed with Taqman RNA to Ct mastermix (Thermo) using the following custom probes (IDT) to determine RNA abundance (Luciferase) and plasmid contamination (Bacterial ORI).

Luciferase:

Probe: 5' FAM-CAGCGACGA/zen/CCTGCCTAAGATGTT-IABkFQ

Primer 1: 5' CACGATAGCGTTGCTGAAGA

Primer 2: 5' CAGATCGTCCGGAAGTACAAC

Bacterial ORI:

Probe: 5' HEX-TTGAAGTGG/zen/TGGCCTAACTACGGC-IABkFQ

Primer 1: 5' GCAGAGCGCAGATACCAAATA

Primer 2: 5' CAGCCACTGGTAACAGGATTA

Fractionation:

3 10cm plates of 293T cells were transfected with 1ug *Mtss1* UTR Luciferase, 3ug *Atnx2* 48 hours before fractionation. 1 hour before harvest, media was changed on cells. Ribosomes were stalled by treating cells with 100ug/ml cycloheximide 5 minutes before harvest. Cells were scraped into lysis buffer: 200U/ml Superase, 20mM DTT, 1% Triton-X 100, 20mM Tris pH 7.5, 100mM KCl, 5mM MgCl₂, 100ug/ml cycloheximide, roche complete mini protease inhibitor tablet, pelleted by centrifuging 8000g 5 minutes. Lysate was normalized by UV 254 absorbance and loaded onto 10%-50% linear sucrose gradients. Gradients were centrifuged 2hrs at 35000rpm in a SW41 rotor. 14 fractions were collected from each gradient using a FoxyR1 collector, and UV254 traces were acquired. For RNA isolation, fractions were treated with TrizolLS (Life), followed by DNase treatment and QRT-PCR.

Ex-vivo Electrophysiology (SCA1)

Solutions

Artificial CSF (aCSF) contained the following (in mM): 125 NaCl, 3.5 KCl, 26 NaHCO₃, 1.25 NaH₂PO₄, 2 CaCl₂, 1 MgCl₂, and 10 glucose. For all recordings, pipettes were filled with internal recording solution containing the following (in mM): 119 K Gluconate, 2 Na gluconate, 6 NaCl, 2 MgCl₂, 0.9 EGTA, 10 HEPES, 14 Tris-phosphocreatine, 4 MgATP, 0.3 tris-GTP, pH 7.3, osmolarity 290 mOsm.

Preparation of brain slices for electrophysiological recordings.

Mice were anesthetized by isoflurane inhalation, decapitated, and the brains were submerged in pre-warmed (33°C) aCSF. Slices were prepared in aCSF containing dasatinib or DMSO and held at 32.5-34°C on a VT1200 vibratome (Leica). Slices were prepared to a thickness of 300 µm. Once slices were obtained, they were incubated in continuously carbogen (95% O₂/5% CO₂)-bubbled aCSF containing DMSO or dasatinib for 45 minutes at 33°C. Slices were subsequently stored in continuously carbon-bubbled aCSF containing DMSO or dasatinib at room temperature until use. For recordings, slices were placed in a recording chamber and continuously perfused with carbogen-bubbled ACSF containing DMSO or dasatinib at 33°C with a flow rate of 2–3 mls/min.

Patch-clamp recordings

Purkinje neurons were identified for patch-clamp recordings in parasagittal cerebellar slices using a 40x water-immersion objective and Eclipse FN1 upright microscope (Nikon) with infrared differential interference contrast (IR-DIC) optics that were visualized using NIS Elements image analysis software (Nikon). Borosilicate glass patch pipettes were pulled with resistances of 3–5 M Ω . Recordings were made 5 hours after slice preparation. Data were acquired using an Axon CV-7B headstage amplifier, Axon Multiclamp 700B amplifier, Digidata 1440A interface, and pClamp-10 software (MDS Analytical Technologies). In all cases, acquired data were digitized at 100 kHz.

QUANTIFICATION AND STATISTICAL ANALYSIS

For cell counts, firing rates, rotorod and activity chamber 2-tailed non-homodidactic Student's T-test was used to calculate significance.

For cerebellar dasatinib cohorts of 2-5 mice were tested. Analysis was T-test with two-stage step-up method of Benjamini, Krieger and Yekutieli with a 1% FDR for multiple test correction.

To compare firing rates and RNAIP 1-way ANOVA followed by Tukey post-hoc testing was used. Luciferase assay was evaluated using two-way ANOVA with reporter construct and co-transfected plasmids as independent variables.

For electrophysiology 2-3 mice per condition were evaluated with investigator blinded to genotype. For MTSS1 rotorod and activity chamber cohorts of 10 age matched animals were examined with investigator blind to genotypes.

For western blots and immune fluorescence 2-5 mice per genotype and age were evaluated.

Figure S1. Sagittal sections of MIM^{EX15} mutants and antibody validation A: mosaic images of 16 week old WT and MIM^{EX15} demonstrate widespread Purkinje neuron loss and increased GFAP staining intensity. B: MTSS1 antibody specificity is shown by lack of signal on MIM^{EX15} tissue. C: Western blot of 4 week cerebella show MIM^{EX15/+} have 25% reduction in MTSS1 compared to WT *p<0.05, **p<0.0001, 1-way ANOVA, Tukey post-hoc test.

Figure S2. Purkinje cell autophagy in MIM^{EX15} mutants

A: Western blot shows no increase in LC3-ii levels in 4 week old MIM^{EX15} mutants. B: *Sqstrm1* (P62) transcript is not increased in MIM^{EX15} mutants and protein levels are not elevated. C: Electron micrographs of 8 week old animals showing defects present in 3 MIM^{EX15} mutants but absent in WT animals: swollen mitochondria where the inner matrix is poorly resolved and dissociated from the outer matrix, electron dense autophagic bodies (AV), lamellar bodies in Purkinje neuron dendrites.

Figure S3. Acute Src inhibition restores tonic firing rates

Average firing frequency measured at the end of each incubation hour of Dasatinib in MIM^{EX15} (A) and ATXN2^{Q127} (B) is plotted. A respective mean value with number of Purkinje neurons (PN) at indicated incubations is given in the figure. Note that baseline firing frequency of ATXN2^{Q127} (14±1 Hz, n=100 PNs) mice of this age is similar to the MIM^{EX15} (12±1 Hz, n=55 PNs). Basal firing frequency of PNs from wild-type mouse are given.

Figure S4. ATXN2 regulates translation through the MTSS1 3'UTR

A: MTSS1 immuno-fluorescence in ATXN2^{Q127} and age matched control mice show reduced Purkinje neuron signal at 4, 12 and 24 week time points. B: Quantitative RT-PCR (QPCR) shows *Mtss1* transcript abundance is reduced in ATXN2^{Q127} compared to age matched controls *p<0.05, **p<0.01, student's t-test, SD error bars. C: RNA-IP followed by QPCR shows ATXN2 binding to the MTSS1 3'UTR is mediated by a central 500bp region *p<0.05 **p=0.015, one-way ANOVA with Tukey post-hoc test. D: Luciferase reporter assay shows ATXN2 translation is strongly mediated by the 3'UTR, and ATXN2^{Q108} allele is sufficient to block activation ns not significant, all other interactions p<0.005. 2way ANOVA finds reporter constructs explain 56% of total variance, differences in response to transfection (pcDNA, ATXN2^{Q22}, ATXN2^{Q22+Q108}) between reporter constructs explains 30% of variance, and different response to transfection (pcDNA, ATXN2^{Q22}, ATXN2^{Q22+Q108}) within a reporter explain 14% of total variance.

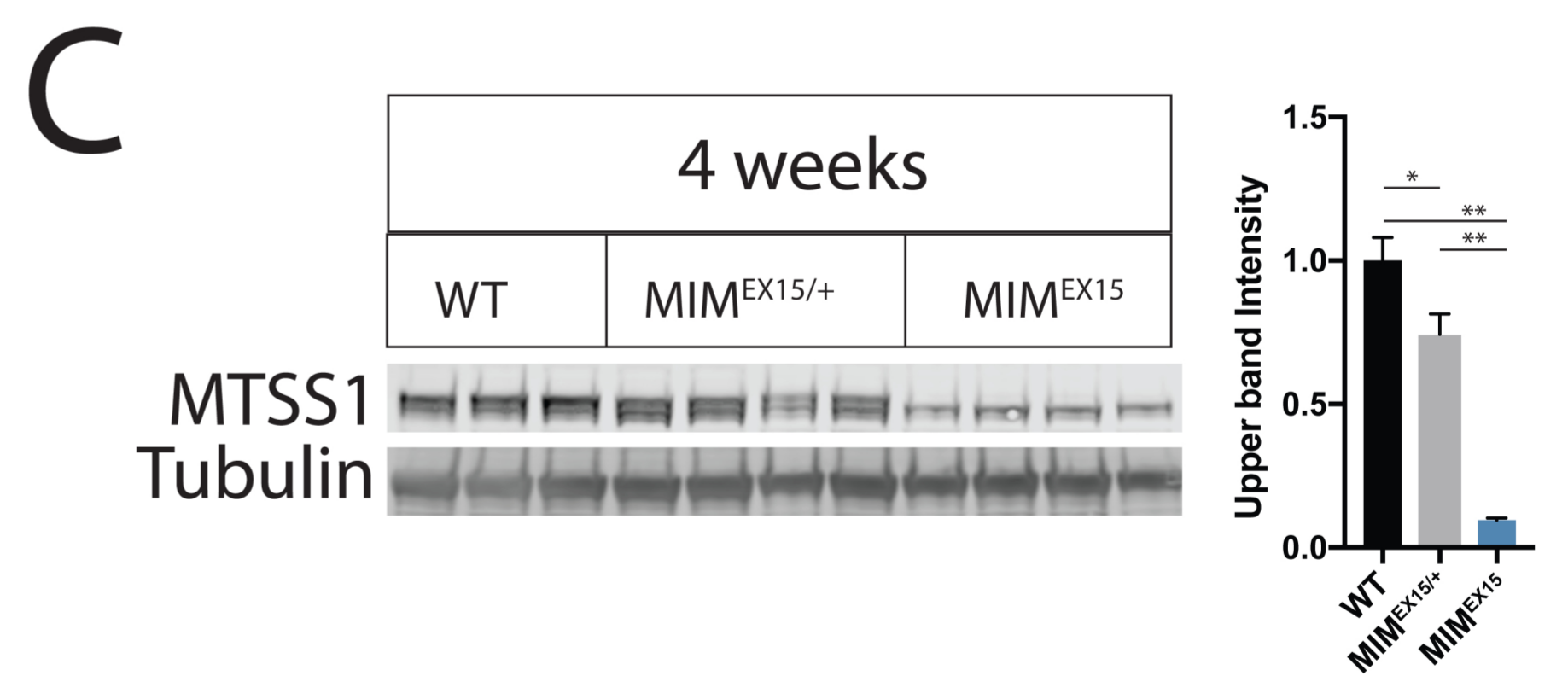
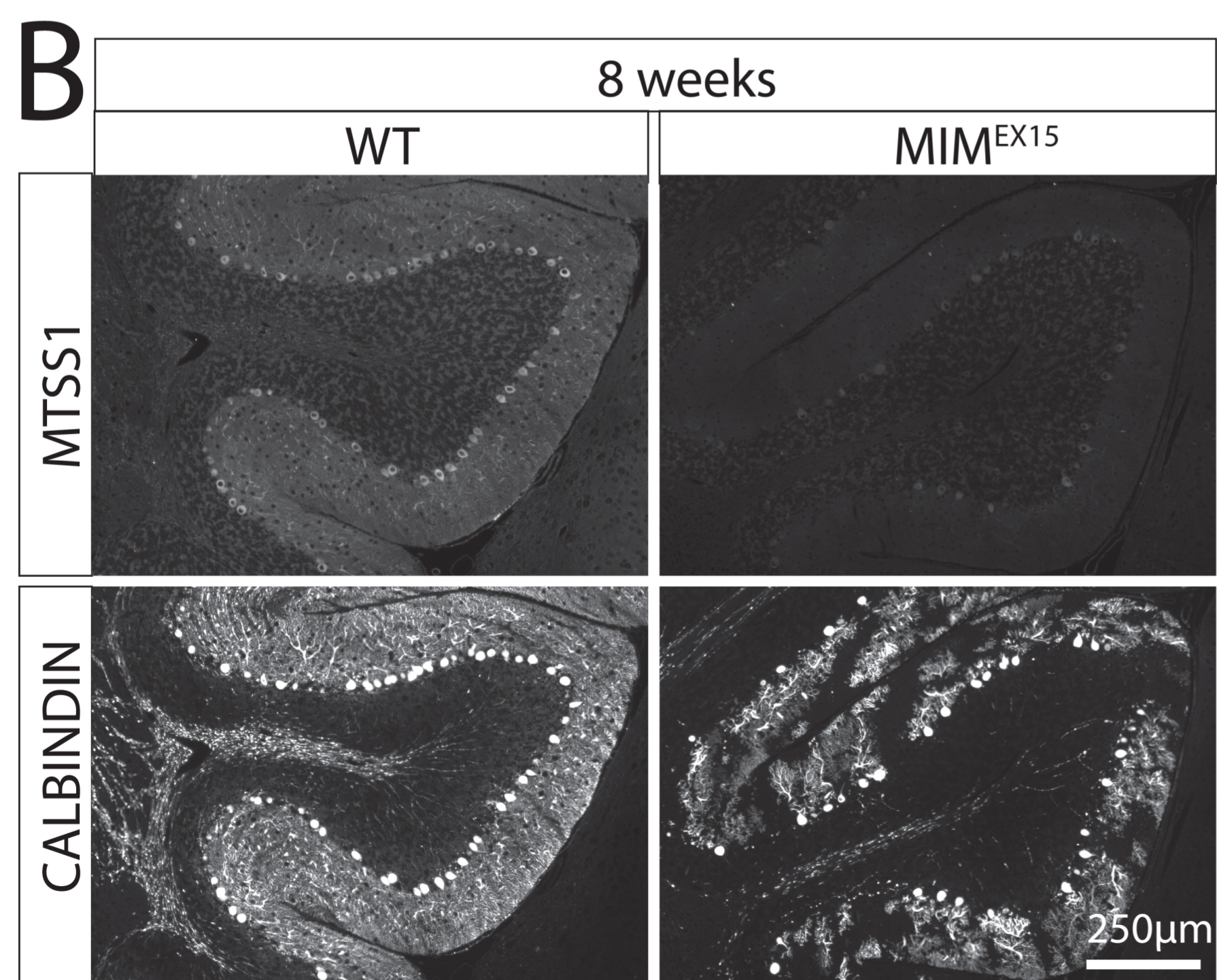
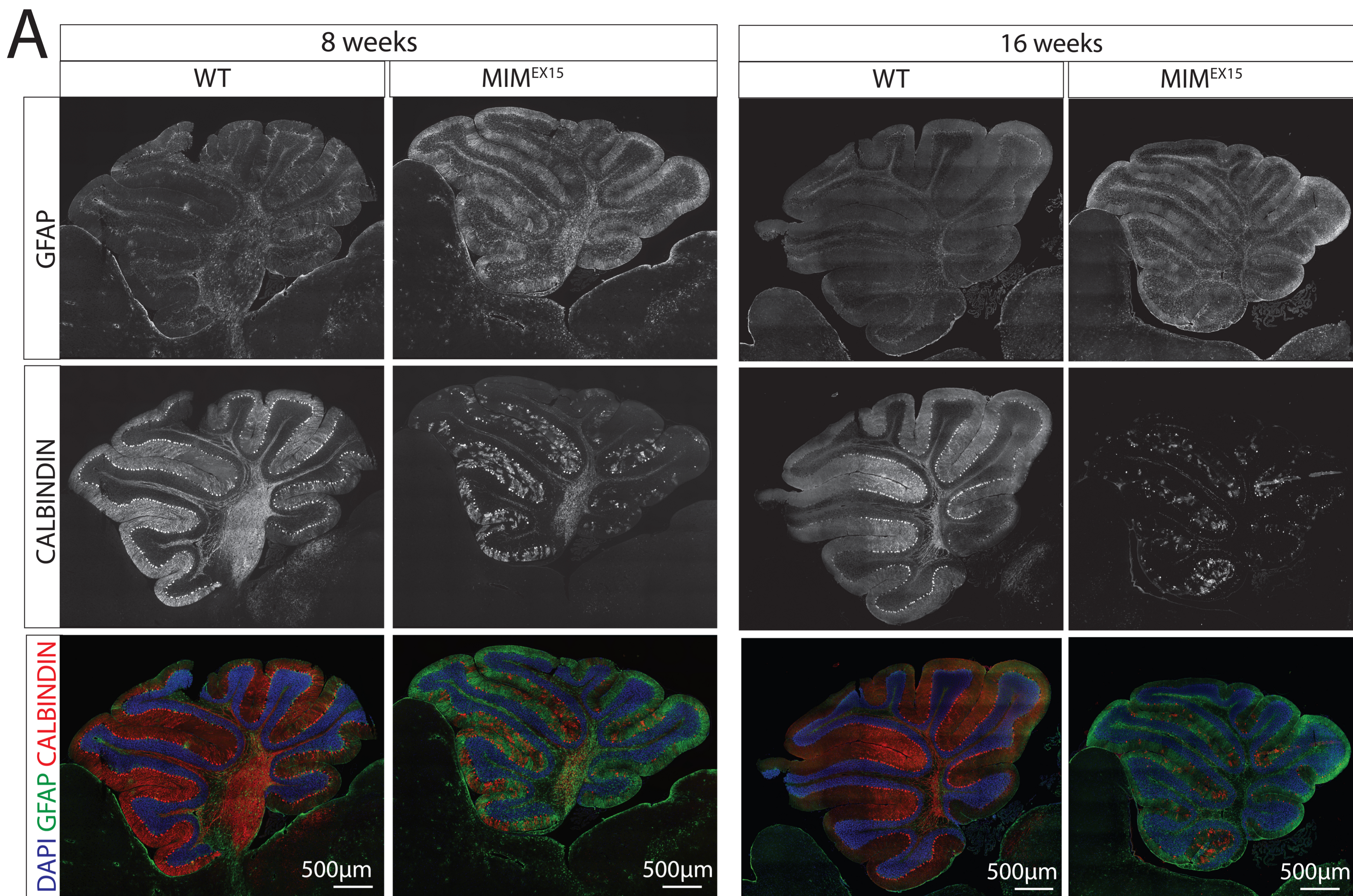


Figure S1

LC3-ii levels

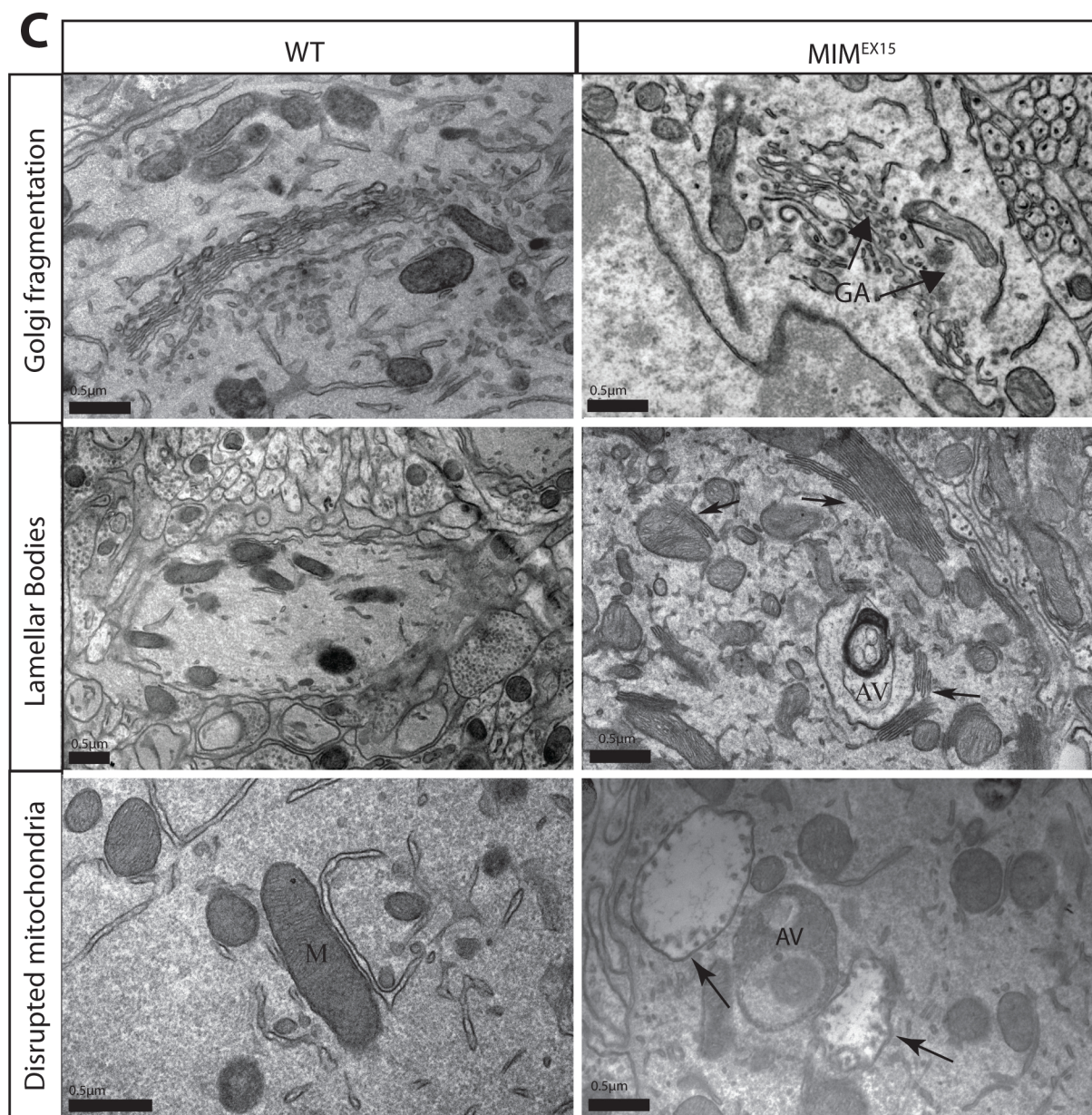
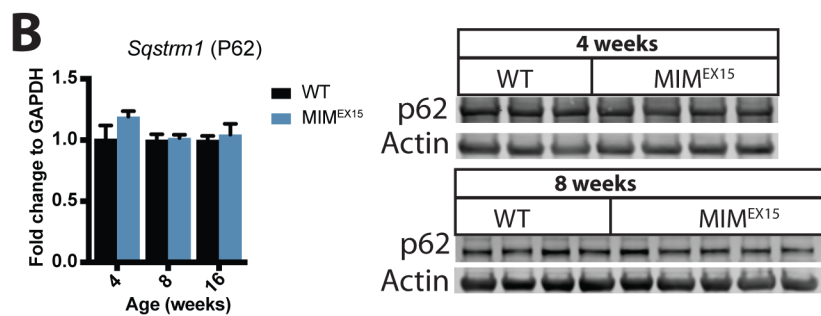
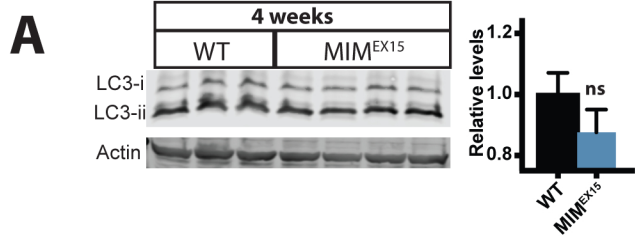


Figure S2

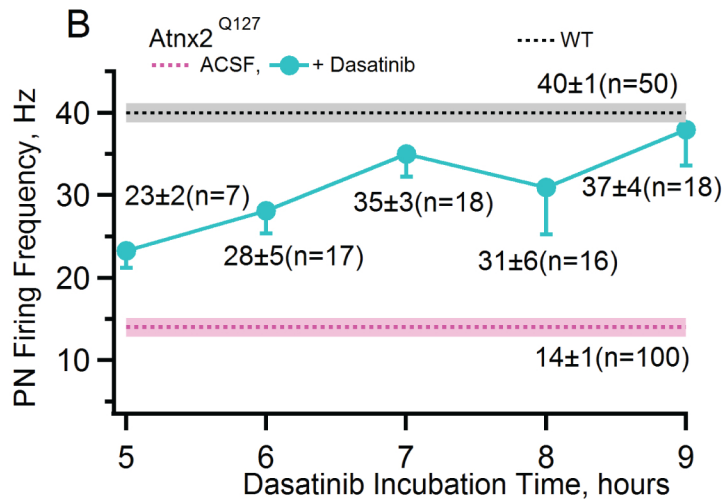
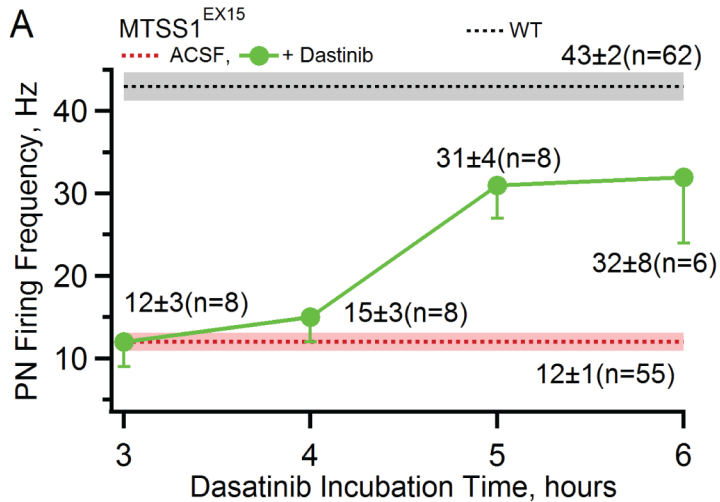


Figure S3

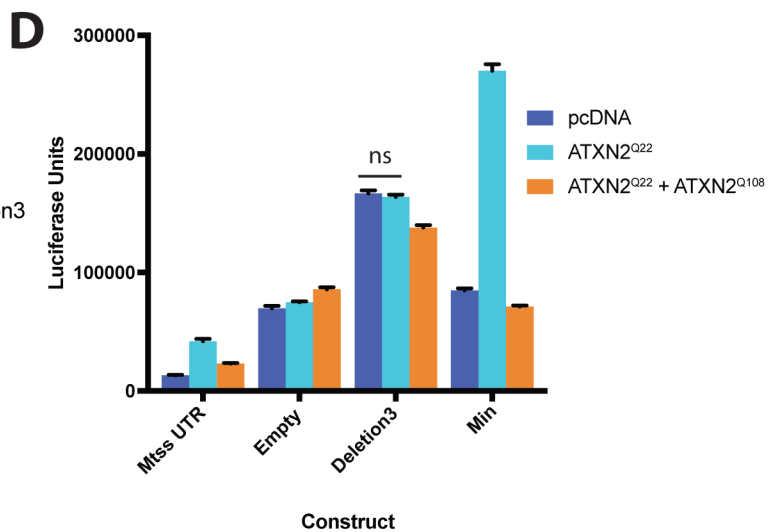
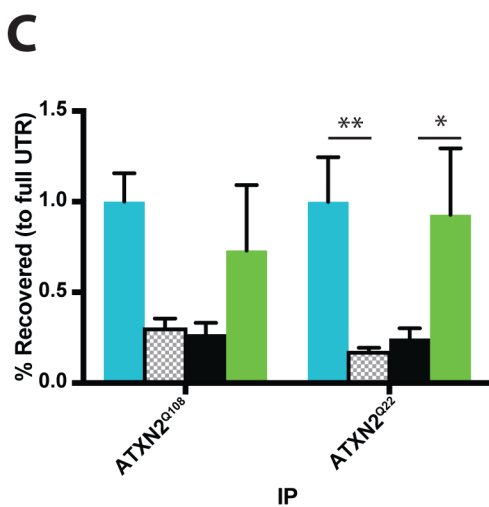
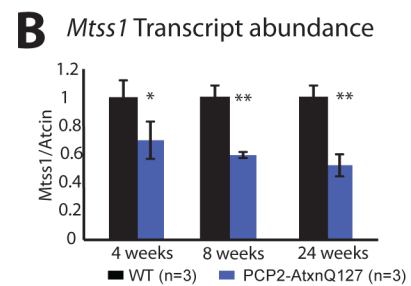
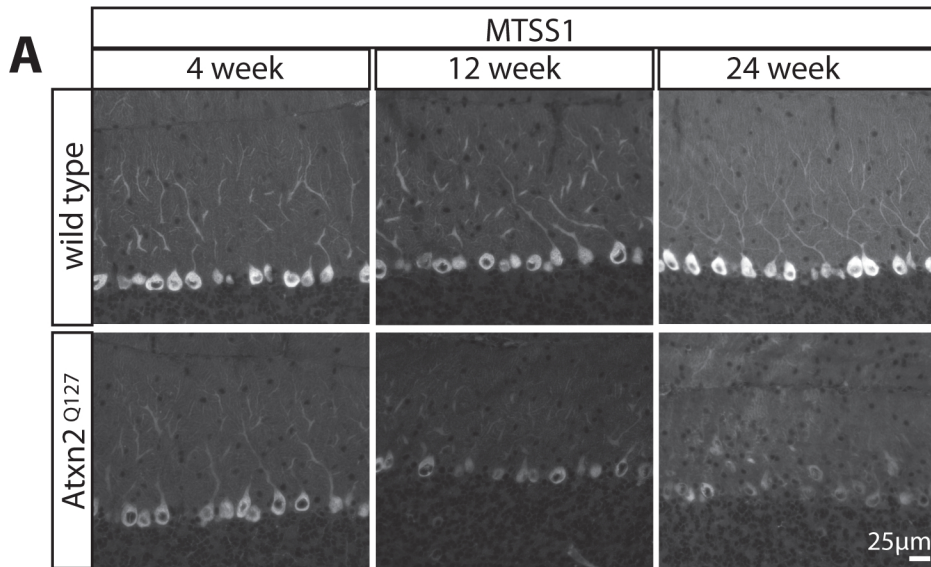


Figure S4